Scattering optics of foam

Moin U. Vera, Arnaud Saint-Jalmes, and Douglas J. Durian

The multiple scattering of light by aqueous foams is systematically studied as a function of wavelength, bubble size, and liquid fraction. Results are analyzed in terms of the transport mean free path of the photons and an extrapolation length ratio for the diffuse photon concentration field. The wavelength dependence is minimal and may be attributed entirely to the wavelength dependence of the refractive index of water rather than thin-film interference effects. The transport mean free path is found to be proportional to the bubble diameter and the reciprocal of the square root of liquid fraction. The extrapolation length ratio varies almost linearly with liquid fraction between the values for water–glass–air and air–glass–air interfaces.

OCIS codes: 080.2710, 170.5280, 170.7050, 030.5620.

1. Introduction

Transparent foams do not exist. Since these materials are composed of gas bubbles packed tightly together in a relatively small volume of soapy water,[1] there are a multitude of gas–liquid interfaces from which light will reflect or refract. For dry foams these interfaces take three forms: the thin soap films separating two bubbles, the scalloped triangular shaped Plateau borders at which three films meet, and the vertices at which four Plateau borders meet. For progressively wetter foams, this distinction gradually vanishes as the borders and vertices inflate and the bubbles become nearly spherical. The same is true for metal or polymer foams, where the scattering is due to gas–solid interfaces with structures similar to those of aqueous foams. In both cases the refractive-index mismatch at the bubble interfaces is large, so multiple scattering is unavoidable.[2] This gives bulk samples their familiar white opaque appearance and prevents optical imaging of interior structures away from the sample boundary, except for foams that are very dry and slowly evolving.[3,4] Multiple scattering also makes whole new classes of foam experiments possible, e.g., Refs. 5–8.

A variety of optical probes have recently been developed for noninvasively probing opaque media. In diffuse-transmission spectroscopy[9] the wavelength-dependent probability for multiply scattered photons to be transmitted through a slab is measured and analyzed in terms of the structures responsible for scattering. In diffusing-wave spectroscopy,[10,11] a photon-correlation technique, temporal fluctuations in the speckle pattern formed by multiply scattered light are measured and analyzed in terms of the dynamics of the scattering sites. Related methods, including optical coherence tomography, have also been developed for reconstructing the spatial dependence of scattering, absorption, and dynamics.[12,13] In all cases quantitative analysis is based on treating photon migration as a diffusion process. Specifically, the concentration field of multiply scattered photons is deduced from a diffusion equation with a diffusion coefficient of $D = cl^*/3$; c is the speed of light between successive scattering events, and l^* is the photon transport mean free path, which can be thought of as the average distance a photon can travel before its direction is randomized. In addition to D, or equivalently l^*, the other important quantity is the extrapolation length ratio z_e, which defines the boundary conditions for the diffusion equation. It is the distance outside the sample, measured in units of l^*, at which the diffuse photon concentration field extrapolates to zero.

In this manuscript we present an experimental study of the dependence of the key photon migration parameters, l^* and z_e, on structure and composition for foams. We find that l^* is proportional to bubble diameter, with a proportionality constant that depends on liquid fraction, and that z_e depends on liquid

At the time this research was performed, the authors were with the Department of Physics and Astronomy, University of California at Los Angeles, Los Angeles, California 90095-1547. A. Saint-Jalmes is now at Laboratoire de Physique des Solides, Université Paris-Sud, 91405 Orsay Cedex, France. D. J. Durian's e-mail address is durian@physics.ucla.edu.

Received 3 November 2000.
0003-6935/01/244210-05$15.00/0

fraction independent of bubble size. These results are consistent with simple considerations of the foam microstructure in terms of scattering by Plateau borders and reflections from the sample boundaries. This understanding can form the basis for future multiple-light-scattering studies of the time evolution of foams and of their microstructural response to shear. For example, the simultaneous measurement of l^*, through light scattering, and of the average bubble size, through direct imaging, may be combined to give the local liquid fraction anywhere within a column of foam and its evolution as the foam drains and coarsens.[14] Conversly, if the liquid fraction is known, then the average bubble size may be deduced. This fulfills the promise[2] of multiple light scattering as a fast, noninvasive, quantitative probe of foam structure.

2. Experimental Procedures

Two very different foaming systems are used in our experiments. In the first, foam is produced by turbulent mixing of gas with a jet of aqueous solution of α-olefinsulfonate (AOS) plus carbopol; see Ref. 15 for the production method and Refs. 16 and 17 for the solution properties. By altering the ratio of gas to liquid flow rate, it is possible to achieve foams with any desired liquid fraction, $0.03 < \varepsilon < 0.50$, with bubbles of 100-μm average diameter. For multiple-light-scattering studies, these foams are loaded into a rectangular cell of thickness $L = 1.17$ cm; the height and width are roughly 20 cm, so large that no light escapes from the edges when the cell is illuminated in the center. In the second system, foam is obtained from a commercial shaving cream, Gillette Foamy Regular, by an aerosol method. In this product the liquid fraction is $\varepsilon \approx 0.08$, and the average bubble diameter is 30 μm. We are able to vary these quantities simultaneously by expanding or compressing the foam in a sealed glass container 40.5-cm tall, 4-cm wide, and $L = 1$ cm thick.

To characterize the optical properties of these foams, we illuminate the central portion of the sample at normal incidence and measure the intensity of both the diffusely transmitted and the diffusely backscattered light as a function of angle. This is accomplished with the apparatus and procedures of Ref. 18, wherein the sample is at the center of a rotation stage and the collection optics are held fixed. Light from either a laser or a combination of a xenon arc lamp plus a monochromator is coupled onto the sample through an optical fiber bundle and lens mounted on the rotation stage. The bandwidth of the monochromator is opened to 10 nm to ensure an easily detectable quantity of light.

The first step in data analysis is to determine the extrapolation length ratio, z_e, from the angular dependence of the diffuse transmission probability. When the boundary consists of a stratified dielectric profile, the diffusion theory prediction is[18]

$$\frac{P(\mu_e)}{\mu_e} = \frac{3}{2}\left(\frac{n_e}{n_i}\right)^2 (z_e + \mu_i)[1 - R(\mu_i)], \qquad (1)$$

where n_i and n_e are the refractive indices of the sample interior and exterior, respectively, $R(\mu_i)$ is the total reflectivity for a photon striking the boundary at an angle $\cos^{-1}(\mu_i)$ from the interior normal, and μ_i and μ_e are related by Snell's law. For foams, photons can strike the boundary from inside a gas bubble or from inside the liquid, so the resulting profile is the sum of two terms like Eq. (1) with different interior indices. This is discussed in Ref. 18 for the commercial shaving foam in a glass cell, where we find $z_e = 1.05$ when the cell is in air and other (consistent) values when the cell is submerged in water or glycerin.

The second step is to extract the transport mean free path, l^*, from the ratio of diffuse transmission to backscattering. These probabilities are found to within the same proportionality constant by integration of the respective angle-dependent intensities. For slabs that are thick enough that essentially no ballistic unscattered light gets through, diffusion theory gives[19]

$$\frac{T_d}{B_d} \approx \frac{\sinh(\sqrt{3\mu_a'})/\sqrt{3\mu_a'} + z_e \cosh(\sqrt{3\mu_a'})}{\sinh[(L' - 1)\sqrt{3\mu_a'}]/\sqrt{3\mu_a'} + z_e \cosh[(L' - 1)\sqrt{3\mu_a'}]}, \qquad (2)$$

where $L' = L/l^*$, $\mu_a' = l^*/l_a$, and l_a is the absorption length. For thinner slabs, or for strong absorption, the prediction is more complex and involves the average cosine of the scattering angle.[19] For our samples, L' is fairly large and μ_a' is very small, so the prediction is not significantly different from the $\mu_a' \to 0$ limit of $T_d/B_d = (1 + z_e)/(L' - 1 + z_e)$. Thus, from relation (2) and the measured value of z_e, we may deduce l^*. A key advantage of this procedure is that normalization and comparison with a standard are unnecessary.

To check our apparatus and analysis procedures, we first examined opaque solutions of polystyrene spheres of diameters 91 and 653 nm, for which l^* can be accurately predicted from Mie theory. The solutions were held in rectangular glass cells of nominal thicknesses of $L = 6, 7, 8, 9$ mm. The concentration of the solutions was chosen so that $l^* \approx 0.5$ mm, at $\lambda = 500$ nm, so that the samples are well into the diffuse limit where relations (1) and (2) apply. For the $D = 91$ nm samples, we find that l^* increases approximately as λ^4 as the wavelength is increased across the visible portion of the spectrum, $400 < \lambda < 800$ nm. For the $D = 653$ nm samples, we find that l^* also increases monotonically, but with a series of bumps and wiggles due to Mie resonances. In all cases the agreement with prediction is quite good, typically 10–20%. This error is systematic (e.g., due to inaccurate values for L) in that it is much larger than the 0.1% scatter between successive data points in a wavelength scan.

Unlike polyball suspensions, aqueous foams are

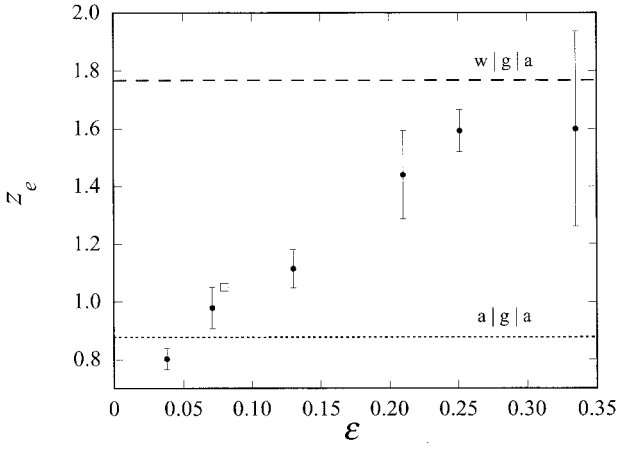

Fig. 1. Extrapolation length ratio versus liquid fraction. Results are obtained from the angular dependence of the diffusely transmitted light. Filled circles are for the AOS foams, and the open square is the value found in Ref. 18 for Gillette Foamy Regular.

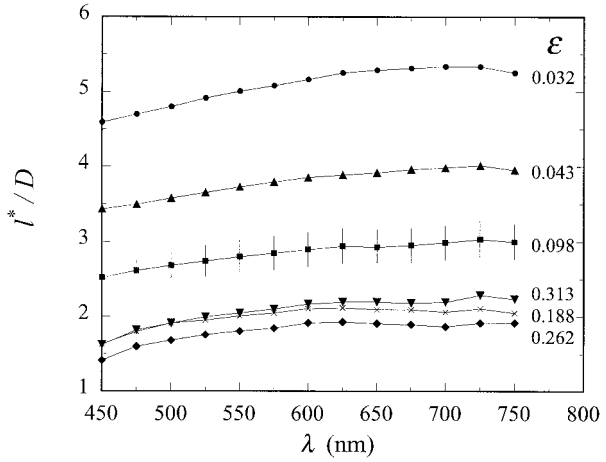

Fig. 2. Ratio of transport mean free path to bubble diameter, versus wavelength, for several different liquid fractions as labeled. The foam samples are made from aqueous solution of AOS and have an average bubble diameter of ~100 μm. The error bars shown for ε = 0.98 indicate systematic errors and are representative of all samples.

nonequilibrium systems. With time, surface tension causes power-law growth of the average bubble size by gas diffusion from smaller to larger bubbles; this is known as coarsening. Furthermore, gravity causes the liquid fraction to change through the flow of liquid through the random interconnected network of Plateau borders. In rectangular cells a drying front starts at the top and moves downward at constant speed; the liquid fraction in the central portion of the sample is constant until this front passes through. To avoid the effects of drainage, we therefore make measurements over a 15–20-min period, before the draining front reaches the scattering volume. To avoid the effects of coarsening is not as simple, since power-law growth means it is faster for younger foams. Therefore we perform 4 or 5 full angular scans and extrapolate back to time zero at each angle. A new sample is thus needed for each wavelength.

3. Extrapolation Length Ratio

Results for the extrapolation length ratio for aqeuous foams, deduced from the angular dependence of the diffusely transmitted light, are shown in Fig. 1 as a function of liquid fraction. Most data points are for the AOS foams, but one is for Gillette Foamy Regular. To within our error bars, there is no discernable wavelength dependence. For dry foams, z_e is close to the value 0.88 for an air (interior)–glass–air (exterior) interface. In this case, the exiting photons strike the boundary almost exclusively from inside gas bubbles pressed up against the glass walls. For wet foams, by contrast, z_e is close to the value 1.77 for a water (interior)–glass–air (exterior) interface. In this case the exiting photons strike the boundary almost exclusively from inside the liquid residing between bubbles. To within the error bars, approximately ±10%, z_e increases linearly with liquid fraction between these two extremes. Some such monotonic trend is to be expected, but there is no obvious reason why it should be almost linear. The results in Fig. 1 should be representative of all aqueous foams, independent of bubble size or species of surfactant. Here they will be used to extract the l^* values presented next.

4. Transport Mean Free Path

Typical results for the transport mean free path, deduced from the ratio of diffusely transmitted to backscattered light by means of relation (2), are shown in Fig. 2 as a function of wavelength. For all the liquid fractions examined, l^* increases monotonically with wavelength across the visible portion of the spectrum. However, this effect is not large—only ~10%. It could be entirely due to the decrease of water's refractive index with wavelength, which would give weaker reflectivities and larger mean free paths. The lack of structure in the l^* versus λ spectrum implies the absence of thin-film interference effects; furthermore, it suggests that the soap films are not the primary source of scattering in foams.

Since to good approximation l^* is independent of λ, we may investigate the dependence on bubble size and liquid fraction at a single fixed wavelength, either 514 or 532 nm. Results for the ratio l^*/D of transport mean free path to average bubble diameter are collected in Fig. 3 as a function of liquid fraction. The first feature to note is that the two data sets collapse onto one universal curve. For the AOS foams, the bubble diameter is constant, ~100 μm; for the expanded or compressed Foamy samples, the diameter is smaller and varies systematically with ε. The agreement in Fig. 3 shows that l^* is indeed proportional to D for all ε. This generalizes on the result $l^* = 3.5D$ found in Ref. 2 for a coarsening foam at a single fixed liquid volume fraction of ε = 0.08. The next feature to note in Fig. 3 is that the value of l^*/D decreases monotonically with increasing ε; in other

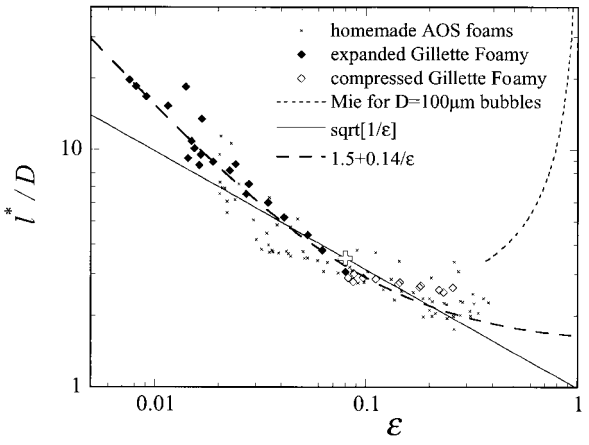

Fig. 3. Ratio of transport mean free path to bubble diameter, versus liquid fraction, for both homemade foams of AOS and Gillette Foamy Regular as labeled. The open plus is for the value observed in Ref. 2. The solid line is the universal scaling function $l^*/D = \sqrt{1/\varepsilon}$, which is predicted to hold for any aqeuous foam in which scattering is dominated by the Plateau borders. The short-dashed curve holds for the Mie regime in which the gas bubbles are spherical and distant from nearest neighbors. The long-dashed curve is an empirical form, $l^*/D = 1.5 + 0.4/\varepsilon$, which describes the full range of data quite well.

words, light is scattered more strongly by wetter foams. The approximate functional form is

$$l^*/D = \sqrt{1/\varepsilon}, \tag{3}$$

which is shown as a solid line in the log–log plot. Data are restricted to $\varepsilon < 0.36$, since this is the point at which the bubbles are randomly close-packed spheres; for larger ε the bubbles are not in contact, and the system is a bubbly liquid or froth in which the bubbles rapidly see the upward. If gravity could be eliminated, and if the bubbles were dilute, $\varepsilon \to 1$, then Mie theory would predict the dashed curve $l^* \propto 1/(1 - \varepsilon)$ shown in Fig. 3. Thus l^*/D must eventually reach a minimum then increase as ε becomes large.

The central experimental result of this paper, Eq. (3), over readily accessible values of ε, can be understood by the following argument in terms of scattering from the Plateau borders. According to transport theory, the scattering mean free path is $l_s = 1/(\rho\sigma)$, where ρ is the number density of scattering sites and σ is their cross section; the transport mean free path is $l^* = l_s/(1 - g)$, where g is the average cosine of the scattering angle. The only assumptions needed about foam structure are that the film thickness is small compared with the radius of curvature r of the Plateau borders and that r is small compared with the sphere-equivalent average diameter D of the cells. In this situation, which is assumed in recent theories of foam drainage,[1,20] the liquid fraction scales as $\varepsilon \propto (r/D)^2$, meaning that the volume of liquid in the Plateau borders is much greater than that in the films and vertices. Therefore the borders will also be the primary source of scattering, with a cross section that scales geometrically as $\sigma \propto rD \propto \sqrt{\varepsilon}D^2$. Next, the number density of borders scales as $\rho \propto 1/D^3$, and g is just a number with no ε or D dependence. Though it has no bearing on the work here, we estimate $g \approx 0.5$ from the angular dependence of scattering by a small sample of extremely dry foam that is nearly transparent. Combining these ingredients, we have $l^* \propto D/\sqrt{\varepsilon}$ as observed in Fig. 3. Deviations from this rule are observed for very dry foams and for very wet foams; deviations may arise from failure of the relation $\varepsilon \propto (r/D)^2$ owing to neglect of liquid in the films and vertices, respectively.

5. Conclusions

We have shown that there is almost no wavelength dependence for either the extrapolation length ratio, z_e, or the transport mean free path, l^*, for aqueous foams. Furthermore, z_e and the ratio l^*/D are independent of bubble diameter D and vary systematically only with the liquid fraction ε of the foam. The specific behavior shown in Figs. 1 and 3 can be understood by simple considerations of the bubble-packing microstructure. This provides the fundamental basis for exploiting multiple light scattering as a fast, noninvasive, quantitative probe of foam structure. For example, the observations in Ref. 14 of the coupling between drainage and coarsening rely crucially on the results presented here. To complement this work, ray-tracing studies of scattering based on a detailed model of foam microstructure would be very interesting. In a slightly different direction, it would be interesting to study absorption of light in a foam as a systematic function of the absorptivity of the surfactant solution. This would reveal the fraction of time migrating photons spend inside the gas bubbles, as opposed to inside the liquid, and might give insight into our z_e versus ε results. We hope the experimental and theoretical protocals developed here for foams may also be helpful for study of other opaque materials with complex microstructures and boundaries, such as polymer foams, granular media, or biological tissues.

This work was supported by NASA though Microgravity Fluid Physics grant NAG3-1419.

References

1. D. Weaire and S. Hutzler, *The Physics of Foams* (Oxford U. Press, New York, 1999).
2. D. J. Durian, D. A. Weitz, and D. J. Pine, "Multiple light scattering probes of foam structure and dynamics," Science **252,** 686–688 (1991).
3. C. Monnereau and M. Vignes-Adler, "Dynamics of 3D real foam coarsening," Phys. Rev. Lett. **80,** 5228–5231 (1998).
4. M. R. Fetterman, E. Tan, L. Ying, R. A. Stack, D. L. Marks, S. Feller, E. Cull, J. M. Sullivan, D. C. Munson, Jr., S. T. Thoroddsen, and D. J. Brady, "Tomographic imaging of foam," Opt. Express **7,** 186–197 (2000), *http://www.opticsexpress.org/oearchive/source/23156.htm.*
5. D. J. Durian, D. A. Weitz, and D. J. Pine, "Scaling behavior in shaving cream," Phys. Rev. A **44,** R7902–R7905 (1991).
6. J. C. Earnshaw and A. H. Jaafar, "Diffusing-wave spectroscopy of a flowing foam," Phys. Rev. E **49,** 5408–5411 (1994).

7. R. Hohler, S. Cohen-Addad, and H. Hoballah, "Periodic nonlinear bubble motion in aqueous foam under oscillating shear strain," Phys. Rev. Lett. **79,** 1154–1157 (1997).
8. A. D. Gopal and D. J. Durian, "Shear-induced 'melting' of an aqueous foam," J. Coll. I. Sci. **213,** 169–178 (1999).
9. P. D. Kaplan, A. D. Dinsmore, A. G. Yodh, and D. J. Pine, "Diffuse-transmission spectroscopy: a structural probe of opaque colloidal mixtures," Phys. Rev. E **50,** 4827–4835 (1994).
10. D. A. Weitz and D. J. Pine, in *Dynamic Light Scattering: The Method and Some Applications*, W. Brown, ed. (Claredon, Oxford, 1993), pp. 652–720.
11. G. Maret, "Diffusing-wave spectroscopy," Curr. Opin. Colloid Interface Sci. **2,** 251–257 (1997).
12. A. G. Yodh and B. Chance, "Spectroscopy and imaging with diffusing light," Phys. Today **48,** 34–40 (1995).
13. J. G. Fujimoto and M. S. Patterson, eds., *Advances in Optical Imaging and Photon Migration* Vol. 21 of OSA Trends in Optics and Photonics (Optical Society of America, Washington, D.C., 1998).
14. M. U. Vera and D. J. Durian, "Gas and liquid transport in foam: the coarsening equation," submitted to Phys. Rev. Lett.
15. A. Saint-Jalmes, M. U. Vera, and D. J. Durian, "Uniform foam production by turbulent mixing: new results on free drainage vs liquid content," Eur. Phys. J. B **12,** 67–73 (1999).
16. P. B. Rand, "Stabilized aqueous foam systems and concentrate and method for making them," U.S. Patent no. 4,442,018 (10 April 1984).
17. A. Saint-Jalmes and D. J. Durian, "Vanishing elasticity for wet foams: equivalence with emulsions and role of polydispersity," J. Rheol. **43,** 1411–1422 (1999).
18. M. U. Vera and D. J. Durian, "The angular distribution of diffusely transmitted light," Phys. Rev. E **53,** 3215–3224 (1996).
19. P.-A. Lemieux, M. U. Vera, and D. J. Durian, "Diffusing-light spectroscopies outside the diffusive limit: the role of ballistic transport and anisotropic scattering," Phys. Rev. E **57,** 4498–4515 (1998).
20. S. A. Koehler, S. Hilgenfeldt, and H. A. Stone, "A generalized view of foam drainage: experiment and theory," Langmuir **16,** 6327–6341 (2000).